# Disturbance Rejection Improvement in Non-Redundant Robot Arms using Bi-articular Actuators

Valerio Salvucci, Sehoon Oh and Yoichi Hori
Department of Electrical Engineering
University of Tokyo, 3-7-1
Hongo Bunkyoku Tokyo, Japan
Email: {valerio, sehoon}@hori.k.u-tokyo.ac.jp, hori@k.u-tokyo.ac.jp

Yasuto Kimura
Department of Advanced Energy Engineering
The University of Tokyo, 5-1-5
Kashiwanoha, Kashiwa, Chiba, Japan
Email: kimura@hori.k.u-tokyo.ac.jp

***Abstract*—Recently, bio-inspired robotic arms equipped with bi-articular muscles, which are actuators that produce torque in two consecutive joints, have been raising interest. Usually bi-articular actuators are present as a redundancy in actuation, which results in advantages such as dramatical increase in range of end effector impedance which can be achieved without feedback, and the ability to produce a homogeneous maximum output force at the end effector. These advantages however are due to the use of bi-articular actuators in addition to the traditional mono-articular ones. Therefore, drawbacks as design complexity and cost are present.**

**In this paper, the role of bi-articular actuators for robot arm that do not present actuator redundancy is investigated. It is shown that for jumping/walking robots, in static conditions the maximum force in the direction parallel to ground is bigger in the configuration with bi-articular actuators. In dynamic conditions, this results in a greater capability of disturbance rejection to forces directed horizontally respect to the ground. As a result, the presence of bi-articular actuators improves the balance capability of jumping/walking robots.**

## I. Introduction

Recently, bio-inspired robotic arms equipped with bi-articular muscles, which are actuators that produce torque in two consecutive joints, have been raising interest both in hardware and control design aspects.

Regarding the hardware design, bi-articular actuators have been realized by means of pneumatic actuators [1], [2], pulleys [3], [4], planetary gears [5], [6], wires [7], [8]. Concerning the kinematics control design for manipulators equipped with bi-articular actuators (i.e. actuator redundancy resolution problem), approaches based on human muscle activation level patterns [3], [9], [10], approaches based on pseudo inverse matrices [4], [11], and approaches based on infinity norm [12], [13] are used.

As for the dynamics control of robotic arm driven by bi-articular actuators, several researches have been focusing on stiffness control for disturbance rejection [4], [14], other researches on efficiency of bi-articular actuators in walking [7] and swimming [8], where researches in which human walking patterns are used as feedforward control strategy for running robots equipped with bi-articular actuators [1].

In all these researches the bi-articular actuators are present as a redundancy in actuation, which results in several important advantages, for example the dramatical increase in range of end effector impedance which can be achieved without feedback [15], and the ability to produce a homogeneous maximum output force at the end effector [16].

However, such important advantages are due to the use of bi-articular actuators in addition to the traditional mono-articular one. Therefore, drawbacks as design complexity and cost are present.

In this paper, we investigate the role of bi-articular actuators for robot arm equipped with as many actuators as joints. Hence, even if the bi-articular actuator is present, there is no actuator redundancy. A planar robot arm with two links and two actuators is taken into account, in two different actuator configurations. The first configuration presents two mono-articular actuators, each actuator produces a torque about each joint. In the second configuration a mono-articular actuator produces torque about the shoulder joint, and a bi-articular one produces the same torque about both shoulder and elbow joints. Both the statics and dynamics resulting in the two actuator configuration are analyzed. It is shown that the presence of bi-articular actuators changes the shape of maximum force at the end effector improving the balance capability of jumping/walking robots.

In section II, the analysis methods to investigate the role of bi-articular actuators in non-redundant robot arm is described. In section III the experimental set up is illustrated. In Section IV, the experimental and simulation results are illustrated and discussed. Finally, in section V, the conclusions.

## II. Analysis methods

A planar robot arm with two links and two actuators is taken into account, in two different actuator configurations.

The first actuator configuration (mono-mono in the following) presents two mono-articular actuators. Each actuator produces a torque about each joint as in Fig. 1. $T_1$ and $T_2$

978-1-4244-9312-8/11/$26.00 ©2011 IEEE

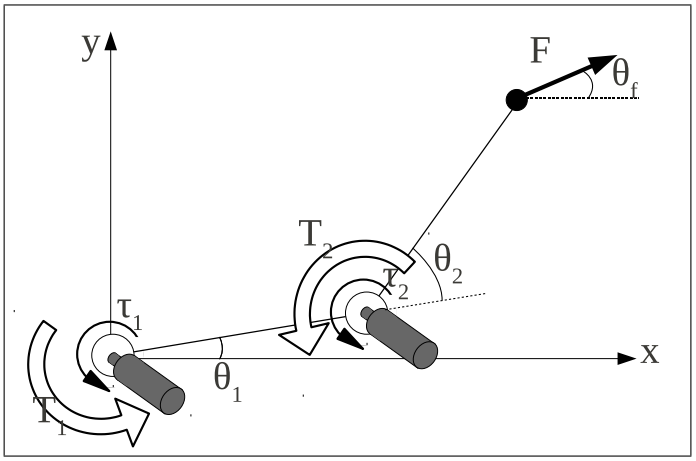


Fig. 1. Robot arm in mono-mono configuration

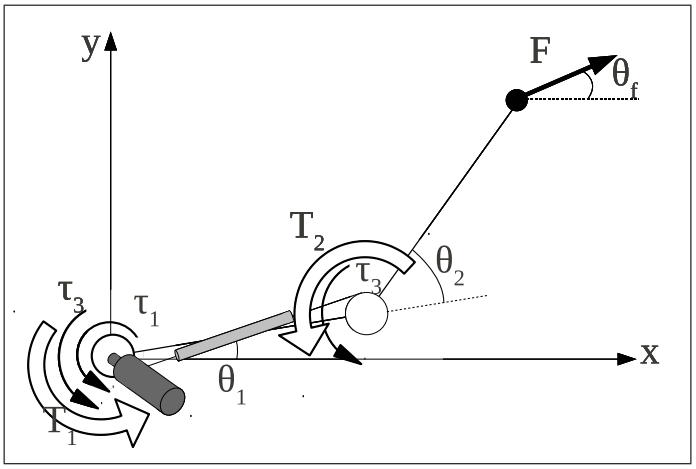


Fig. 2. Robot arm in mono-bi configuration

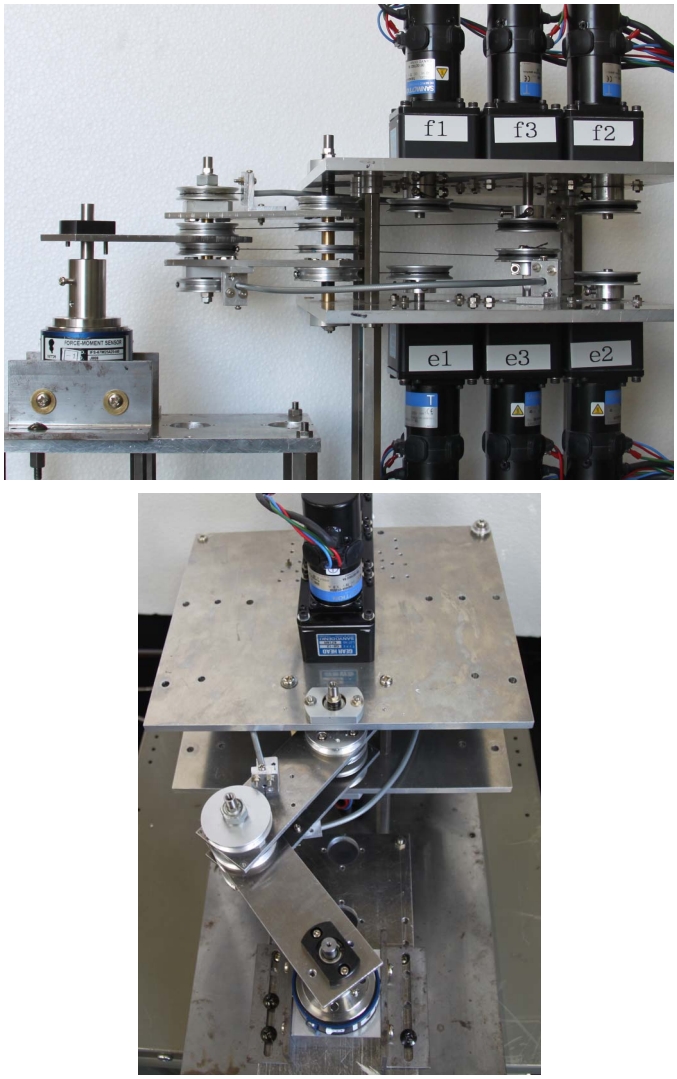


Fig. 3. Mono and bi-articularly actuated, and wire driven robotic arm

are the joint torques. $\tau_1$ and $\tau_2$ are the torques produced on joints 1 and 2 by actuators 1 and 2 respectively. The statics of mono-mono configuration are expressed by:

$$\begin{cases} T_1 = \tau_1 \\ T_2 = \tau_2 \end{cases} \quad (1)$$

In the second configuration (mono-bi in the following), one mono-articular actuator produces a torque on the shoulder joint, and one bi-articular produces the same joint torque about both shoulder and elbow joints, as in Fig.2. $T_1$ and $T_2$ are the joint torques. $\tau_1$ is the torque produced about joint 1 by actuator 1, while $\tau_3$ is the torque produced at the same time about joint 1 and 2 by the bi-articular actuator. The statics of mono-mono configuration are expressed by:

$$\begin{cases} T_1 = \tau_1 + \tau_3 \\ T_2 = \tau_3 \end{cases} \quad (2)$$

Both the statics and dynamics resulting in the two actuator configurations are analyzed in the following.

For the static conditions the maximum output force at the end effector is analyzed in three posture by both calculation and experimental results. The advantages in terms of maximum force production at the end effector when using the bi-articular actuators are highlighted.

Regarding the dynamic aspects, the two configurations are compared by simulation. Due to the capability of the mono-bi configuration in producing higher horizontal force, stronger disturbances on the horizontal direction can be rejected in walking/jumping robot which make use of bi-articular actuators. Such results are in accordance with the experimental results obtained in static conditions.

## III. Experimental Setup

The robot arm used in the experiment is shown in Fig. 3 The two-link planar manipulator has 6 motors, each one representing one of the muscles in Fig. 4.

The power is transmitted to the joints through pulleys and polyethylene wires as shown in Fig. 5:

- A pair of antagonistic mono-articular motors ($e_1$–$f_1$) are connected by mean of polyethylene wires to 2 pulleys

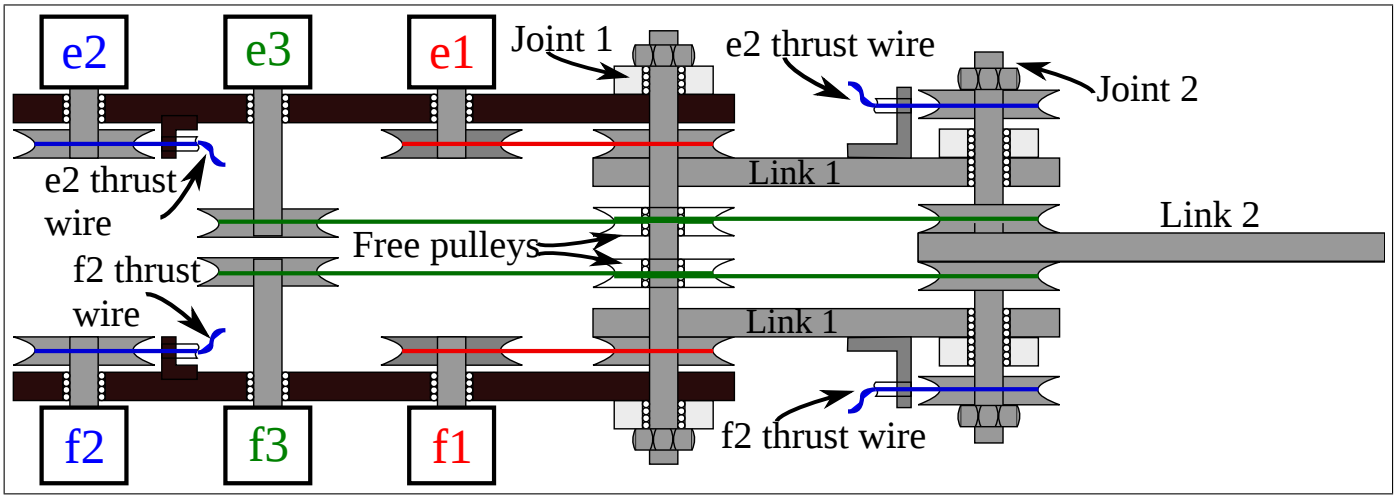


Fig. 5. Torque transmission system

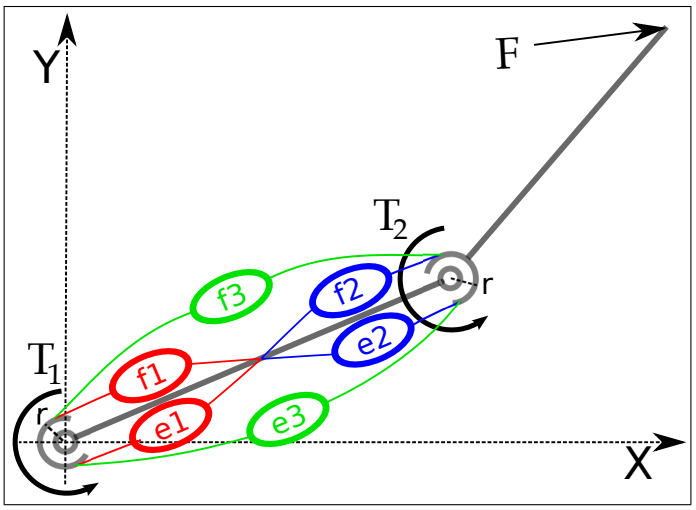


Fig. 4. Scheme a two-link arm with 4 mono- and 2 bi-articular actuators

fixed on joint 1. This motor pair produces the torque $\tau_1$ about joint 1 as in Fig. 4.

- A pair of antagonistic mono-articular motors ($e_2$–$f_2$) are connected by thrust wires to 2 pulleys fixed on joint 2. This motor pair produces the torque $\tau_2$ about joint 2 as in Fig. 4.
- A pair of antagonistic bi-articular motors ($e_3$–$f_3$) are connected by mean of polyethylene wires to pulleys fixed on joint 2, and to free pulleys about joint 1. This motor pair produces the torque $\tau_3$ about joint 1 and 2 as in Fig. 4.

Further characteristics of the proposed manipulator and of the actuator and sensor systems are shown in Tab. I and Tab. II, respectively.

Torque control is realized using the feedforward control strategy in Fig. 6 and Fig. 7 for the mono-mono and mono-bi configurations, respectively.

TABLE I
MANIPULATOR CHARACTERISTICS

| Parameter | value |
|---|---|
| Link 1 | 112 [mm] |
| Link 2 | 112 [mm] |
| Pulleys diameter (all) | 44 [mm] |
| Thrust wires | 30 [mm] |

TABLE II
ACTUATOR AND SENSOR SYSTEM

| | |
|---|---|
| Motors | Sanyo T404-012E59 |
| Gear head | G6-12 (ratio 12.5) |
| Servo system | TS1A02AA |
| Force sensor | Nitta IFS-67M25A25-I40 |

$F_x^*$ and $F_y^*$ are the desired force at the end effector. $J$ is the manipulator Jacobian. $T_1^*$ and $T_2^*$ are the desired joint torques. $\tau_1^*$, $\tau_2^*$ and $\tau_3^*$ are the desired actuator joint torques. As for the torque saturation conditions, in the mono-mono configuration the following algorithm is used:

$$\begin{aligned}&\tau_i^* = T_i^*\\ &\text{if } \tau_i^* > \tau_i^{max},\ \tau_i^* = \tau_i^{max}\\ &\text{if } \tau_i^* < -\tau_i^{max},\ \tau_i^* = -\tau_i^{max}\end{aligned}$$

where $i \in \{1,2\}$. While in the mono-bi configuration the following algorithm is used:

$$\begin{aligned}&\tau_3^* = T_2^*\\ &\text{if } \tau_3^* > \tau_3^{max},\ \tau_3^* = \tau_3^{max}\\ &\text{if } \tau_3^* < -\tau_3^{max},\ \tau_3^* = -\tau_3^{max}\\ &\tau_1^* = T_1^* - \tau_3^*\\ &\text{if } \tau_1^* > \tau_1^{max},\ \tau_1^* = \tau_1^{max}\\ &\text{if } \tau_1^* < -\tau_1^{max},\ \tau_1^* = -\tau_1^{max}\end{aligned}$$

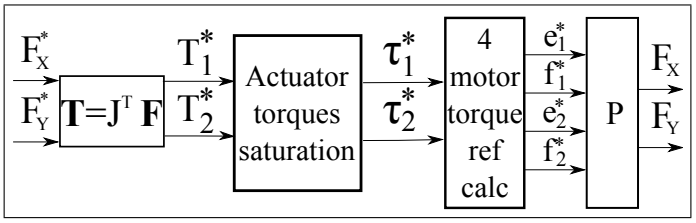


Fig. 6. Feedforward control block diagram for mono-mono configuration

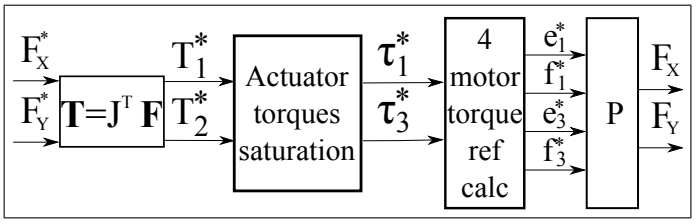


Fig. 7. Feedforward control block diagram for mono-bi configuration

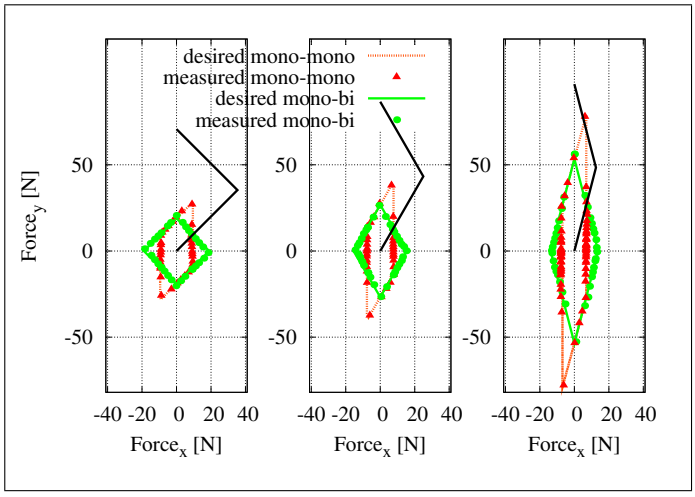


Fig. 8. Experimentally measured maximum output force at the end effector

The motor reference torques are calculated as:

$$e_1^* = \begin{cases} \tau_1^* & if\ \tau_1^* < 0 \\ 0 & \text{otherwise} \end{cases} \quad (3)$$

$$f_1^* = \begin{cases} \tau_1^* & if\ \tau_1^* > 0 \\ 0 & \text{otherwise} \end{cases} \quad (4)$$

$$e_2^* = \begin{cases} K_{tl}\tau_2^* & if\ \tau_2^* < 0 \\ 0 & \text{otherwise} \end{cases} \quad (5)$$

$$f_2^* = \begin{cases} K_{tl}\tau_2^* & if\ \tau_2^* > 0 \\ 0 & \text{otherwise} \end{cases} \quad (6)$$

$$e_3^* = \begin{cases} \tau_3^* & if\ \tau_3^* < 0 \\ 0 & \text{otherwise} \end{cases} \quad (7)$$

$$f_3^* = \begin{cases} \tau_3^* & if\ \tau_3^* > 0 \\ 0 & \text{otherwise} \end{cases} \quad (8)$$

In order to compensate for the inevitable transmission loss in the thrust wires the reference motor torques for joint 2 – $e_2^*$ and $f_2^*$ – are multiplied by a constant $K_{tl} = 1.33$. As results from (3)-(8) the antagonistic actuators are never activated at the same time. Therefore, joint stiffness control is not considered in this study.

In the experiment the arm posture is varied. Three different joint angle configurations are taken into account:

1) $\theta_1 = -135^\circ$ and $\theta_2 = 90^\circ$
2) $\theta_1 = -120^\circ$ and $\theta_2 = 60^\circ$
3) $\theta_1 = -104.5^\circ$ and $\theta_2 = 29^\circ$

The output force is measured for the output force direction ($\theta_f$) varying from 0 to 360° every 10°. The maximum actuator joint torques are set to $\tau_1 = \tau_2 = \tau_3 = 1.5\ Nm$. The motor torque references are sent as step inputs, the manipulator end effector output force $[f_x, f_y]$ is measured by a force sensor, and its steady state value is taken into account.

## IV. Results

### A. Static Analysis

For both the configurations of Fig. 1 and Fig 2 the relationship between force at the end effector and joint torques is expressed by:

$$\begin{bmatrix} T_1 \\ T_2 \end{bmatrix} = J^T \begin{bmatrix} f_x \\ f_y \end{bmatrix} \quad (9)$$

where

$$J = \begin{bmatrix} -l_1\sin(\theta_1) - l_2\sin(\theta_1+\theta_2) & -l_2\sin(\theta_1+\theta_2) \\ l_1\cos(\theta_1) + l_2\cos(\theta_1+\theta_2) & l_2\cos(\theta_1+\theta_2) \end{bmatrix} \quad (10)$$

The main difference for the two configuration are the maximum joint torques $T_1^{max}$ and $T_2^{max}$. In mono-mono configuration the maximum joint torques are:

$$\begin{cases} T_1^{max} = \tau_1^{max} \\ T_2^{max} = \tau_2^{max} \end{cases} \quad (11)$$

In mono-bi configuration the maximum joint torques are:

$$\begin{cases} T_1^{max} = \tau_1^{max} + \tau_3^{max} \\ T_2^{max} = \tau_3^{max} \end{cases} \quad (12)$$

From (12) results that, if the required actuator torques $\tau_1^{max}$ and $\tau_3^{max}$ have opposite sign $T_1^{max}$ is smaller in mono-bi configuration. On the contrary $T_1^{max}$ in mono-bi configuration is greater than in mono-mono configuration when $\tau_1^{max}$ and $\tau_3^{max}$ have same sign.

The sign relationship between $\tau_1^{max}$ and $\tau_3^{max}$ depends on the robot arm posture ($\theta_1$ and $\theta_2$ and on the desired force direction at the end effector ($\theta_f$). As a consequence the maximum output force at the end effector has a different shape in the two actuators configurations.

Maximum output force experimentally measured using the robot arm described in Section III are shown in Fig. 8. Arm postures are $\theta_1 = -135$ and $\theta_2 = 90$, $\theta_1 = -120$ and $\theta_2 = 60$, and $\theta_1 = -104.5$ and $\theta_2 = 29$. The maximum force at the end effector in the direction perpendicular to ground is the same in the two cases. On the

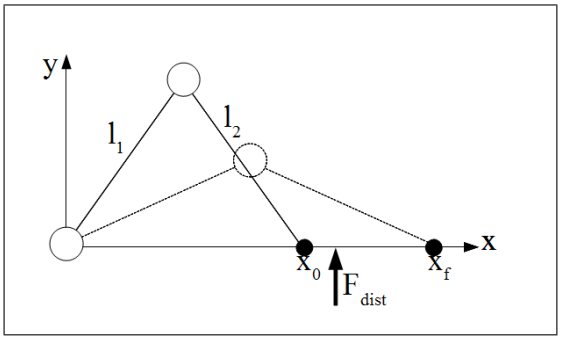


Fig. 9. Arm in initial and desired final position

TABLE III
SIMULATION PARAMETERS

| Parameter | value |
|---|---|
| Length link 1 | 1 $[m]$ |
| Lenght link 2 | 1 $[m]$ |
| Mass 1 | 5 $[Kg]$ |
| Mass 2 | 5 $[Kg]$ |
| COM 1 | 0.5 $[m]$ |
| COM 2 | 0.5 $[m]$ |
| Momentum of Inertia 1 | 2.25 $[Kg/m^2]$ |
| Momentum of Inertia 2 | 2.25 $[Kg/m^2]$ |
| Damping Coefficient Joint 1 | 0.01 $[Ns/m]$ |
| Damping Coefficient Joint 2 | 0.01 $[Ns/m]$ |
| $\tau_1^{max} = \tau_2^{max} = \tau_3^{max}$ | 1 $Nm$ |

other hand, the maximum force in the horizontal direction is bigger in the mono-bi configuration. The possibility of producing a higher force in the horizontal plane is a key aspect for balance of jumping/walking robots.

### B. Dynamic Analysis

In order to investigate the role of bi-articular actuators for non-redundant manipulators in dynamic conditions the following simulation is performed. A two-link planar with $l_1 = l_2 = 1\ m$ is considered (Fig. 9).

The arm initial position is $x(t_0) = 1\ m$, $y(t_0) = 0$. The desired final position is $x(t_f) = 1.8\ m$, $y(t_f) = 0$. The arm in the initial and desired final position is shown in Fig. 9.

A straight trajectory in the Cartesian space is designed using a cubic spline:

$$\begin{cases} x(t) = x_0 + \frac{3}{t_f^2}(x_f - x_0)t^2 - \frac{2}{t_f^3}(x_f - x_0)t^3 \\ y(t) = 0 \end{cases} \quad (13)$$

where $t$ is the time, $t_0 = 0$, $t_f = 5$ seconds.

A disturbance force with magnitude $f_x = 0$, and $f_y = 3.5\ N]$ is applied at $t = 3\ s$ for a length of 0.5 seconds at the end effector. Further parameters used in the simulation are shown in Tab. IV-B.

Fig. 10 shows the control block diagram used in the simulation. P includes all the robot arm dynamics. Joint position control is realized by a PID controller. The tracking performances of the arm in Fig. 9 are evaluated in the two actuator configurations mono-mono and mono-bi. The actuator torque saturation algorithms are (11) for the mono-mono configuration and (12) for the mono-bi configuration.

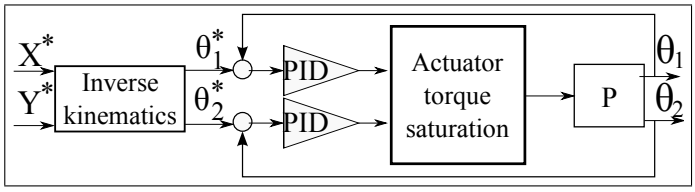


Fig. 10. Control block diagram used in the dynamics simulation

The tracking performances of the arm are shown in Fig. 11 for the mono-mono configuration, and in Fig. 12 for the bi-mono configuration. In particular, desired joint angular positions ($\theta_1^*$ and $\theta_2^*$), actual joint angular positions ($\theta_1$ and $\theta_2$), angular position errors ($\theta_1^{err}$ and $\theta_2^{err}$), desired joint torques ($T_1^*$ and $T_2^*$) and actual joint torques ($T_1$ and $T_2$) are shown.

These results show that in the mono-mono configuration the system is unstable, as the angular position error $\theta_1^{err}$ does not converge to 0. On the other hand, in the mono-bi configuration the position errors $\theta_1^{err}$ and $\theta_2^{err}$ converge to 0. Therefore the arm can reach the final desired position.

## V. CONCLUSION

In this paper, the role of bi-articular actuators for robot arm that do not present actuator redundancy is investigated. A planar robot arm with two links and two actuators is taken into account, in two different actuator configurations.

The first configuration presents two mono-articular actuators (one on each joint), while the second configuration presents a mono-articular actuator on the shoulder joint and a bi-articular one spanning both shoulder and elbow joints. Both the statics and dynamics resulting in the two actuator configurations are investigated.

In static conditions the maximum force at the end effector in the direction perpendicular to ground is the same in the two actuator configuration. On the other hand, the maximum force in the horizontal direction is bigger in the mono-bi configurations.

In dynamic conditions, the greater maximum force in the horizontal direction results in a greater capability of disturbance rejection to forces directed horizontally respect to the ground for jumping/walking robots. As a consequence the presence of bi-articular actuators improve the balance capability of jumping/walking robots.

## REFERENCES

[1] R. Niiyama and Y. Kuniyoshi, "Design principle based on maximum output force profile for a musculoskeletal robot," *Industrial Robot: An International Journal*, vol. 37, no. 3, 2010.

[2] K. Hosoda, Y. Sakaguchi, H. Takayama, and T. Takuma, "Pneumatic-driven jumping robot with anthropomorphic muscular skeleton structure," *Autonomous Robots*, vol. 28, no. 3, pp. 307–316, 2009.

[3] T. Tsuji, "A model of antagonistic triarticular muscle mechanism for lancelet robot," in *The 11th IEEE International Workshop on Advanced Motion Control*, 2010.

[4] K. Yoshida, N. Hata, S. Oh, and Y. Hori, "Extended manipulability measure and application for robot arm equipped with bi-articular driving mechanism," in *35th Annual Conference of the IEEE Industrial Electronics Society, IECON*, 2009.

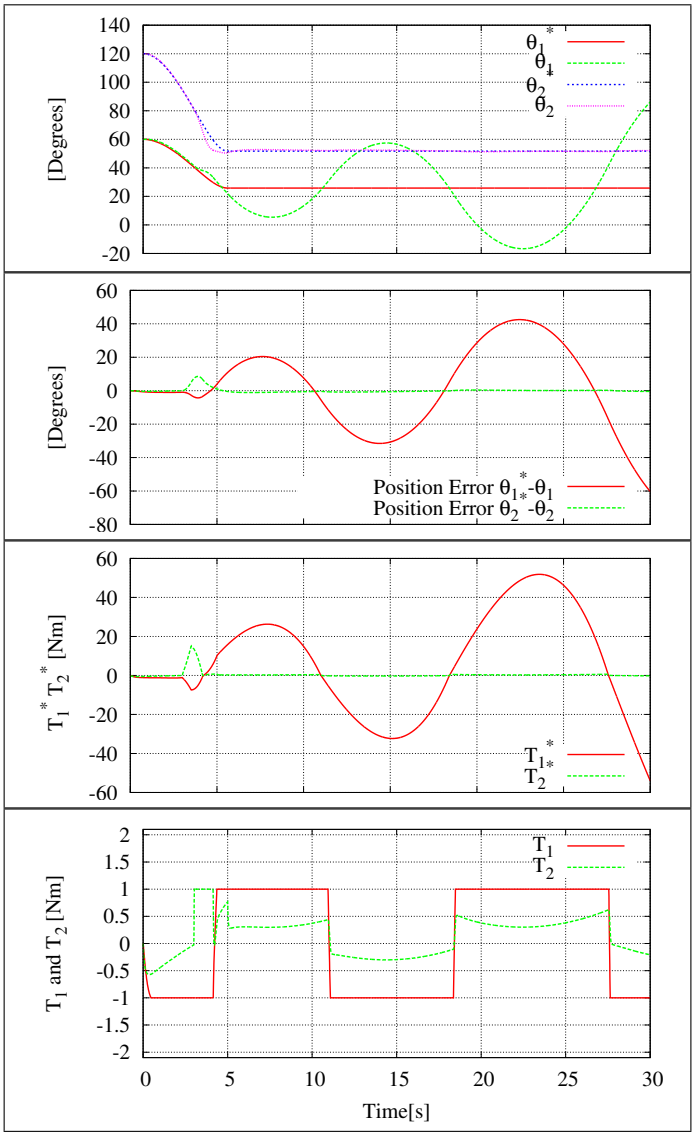


Fig. 11. Tracking performances of the arm in mono-mono configuration

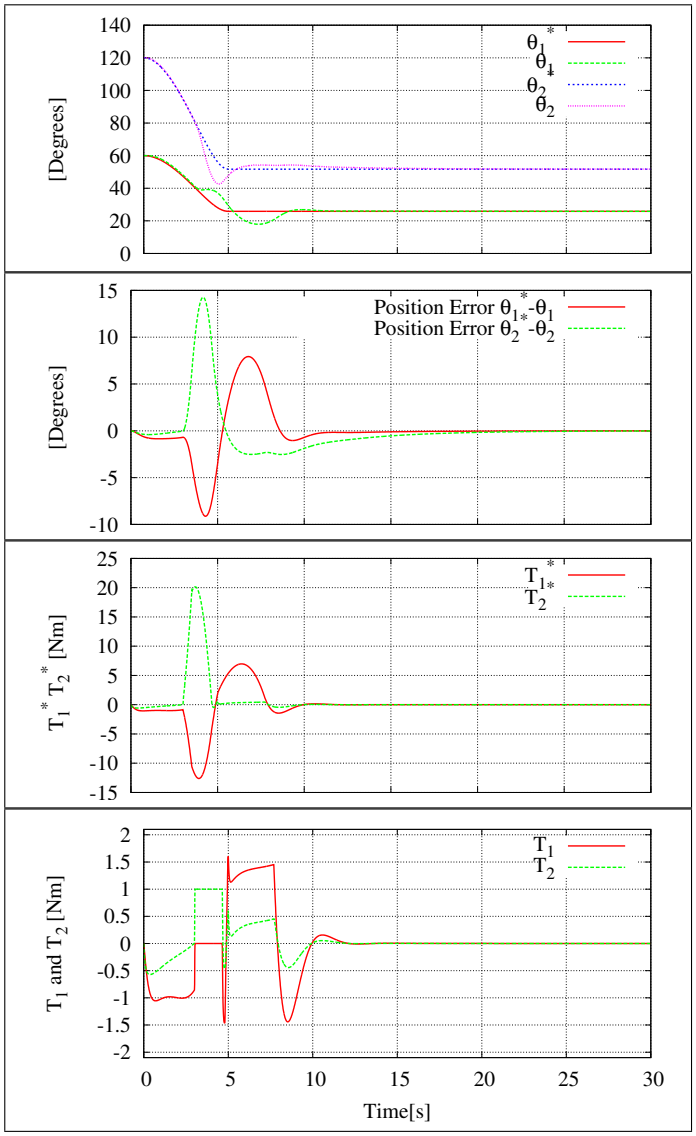


Fig. 12. Tracking performances of the arm in mono-bi configuration


[5] A. Umemura, Y. Saito, and T. Haneyoshi, "The rigidity of the bi-articular robotic arm with a planetary gear," in *Advanced Motion Control, 2010 11th IEEE International Workshop on*, 2010, pp. 490–495.

[6] Y. Kimura, S. Oh, and Y. Hori, "Novel Robot Arm with Bi-articular Driving System Using a Planetary Gear System," in *The 11th IEEE International Workshop on Advanced Motion Control*, 2010.

[7] A. Seyfarth, F. Iida, R. Tausch, M. Stelzer, O. von Stryk, and A. Karguth, "Towards bipedal jogging as a natural result of optimizing walking speed for passively compliant Three-Segmented legs," *The International Journal of Robotics Research*, vol. 28, no. 2, pp. 257 –265, Feb. 2009.

[8] M. A. Lewis and T. J. Klein, "Achilles: A robot with realistic legs," *IEEE Biomedical Circuits and Systems Conference (BIOCAS)*, 2008.

[9] T. Oshima, T. Fujikawa, O. Kameyama, and M. Kumamoto, "Robotic analyses of output force distribution developed by human limbs," in *Robot and Human Interactive Communication, 2000. RO-MAN 2000. Proceedings. 9th IEEE International Workshop on*, 2000, pp. 229–234.

[10] H. Fukusho, T. Koseki, and T. Sugimoto, "Control of a straight line motion for a Two-Link robot arm using coordinate transform of bi-articular simultaneous drive," in *The 11th IEEE International Workshop on Advanced Motion Control*, Japan, 2010.

[11] A. Z. Shukor and Y. Fujimoto, "Modelling and Control of Redundant Robot Manipulator Using Spiral Motor," in *6th Europe-Asia Congress on Mechatronics, EAM*, 2010.

[12] V. Salvucci, S. Oh, and Y. Hori, "Infinity Norm Approach for Precise Force Control of Manipulators Driven by Bi-articular Actuators," in *36th Annual Conference of IEEE Industrial Electronics Society, IECON*, 2010.

[13] ——, "Infinity Norm Approach for Output Force Maximization of Manipulators Driven by Bi-articular Actuators," in *6th Europe-Asia Congress on Mechatronics, EAM*, 2010.

[14] S. Oh, Y. Kimura, and Y. Hori, "Reaction Force Control of Robot Manipulator Based on Biarticular Muscle Viscoelasticity Control," in *IEEE International Conference on Advanced Intelligent Mechatronics*, 2010.

[15] N. Hogan, "Impedance control: An approach to manipulation: Part II—Implementation," *Journal of Dynamic Systems, Measurement, and Control*, vol. 107, no. 1, pp. 8–16, Mar. 1985.

[16] T. Fujikawa, T. Oshima, M. Kumamoto, and N. Yokoi, "Output force at the endpoint in human upper extremities and coordinating activities of each antagonistic pairs of muscles," *Transactions of the Japan Society of Mechanical Engineers*, 1999, [In Japanese].